MOUND CRATERS ON RUBBLE-PILE BENNU INDICATE STRENGTH AT DEPTH. R. T. Daly[1], E. B. Bierhaus[2], O. S. Barnouin[1], M. G. Daly[3], J. A. Seabrook[3], J. H. Roberts[1], C. M. Ernst[1], M. E. Perry[1], H. Nair[1], R. C. Espiritu[1], E. E. Palmer[4], R. W. Gaskell[4], J. R. Weirich[4], H. C. M. Susorney[5], C. L. Johnson[5,6], K. J. Walsh[7], M. C. Nolan[8], E. R. Jawin[9], P. Michel[10], D. Trang[11], and D. S. Lauretta[8]. [1]Johns Hopkins University Applied Physics Laboratory, Laurel, MD, USA (terik.daly@jhuapl.edu); [2]Lockheed Martin Space, Littleton, CO, USA; [3]Centre for Research in Earth and Space Science, York University, Toronto, Ontario, Canada; [4]Planetary Science Institute, Tucson, AZ, USA; [5]School of Earth Sciences, University of Bristol, Bristol, UK; [6]Dept. of Earth, Ocean & Atmospheric Sciences, University of British Columbia, Vancouver, Canada; [7]Southwest Research Institute, Boulder, CO, USA; [8]Lunar and Planetary Laboratory, University of Arizona, Tucson, AZ, USA; [9]Smithsonian Institution National Museum of Natural History, Washington, D.C., USA; [10]Université Côte d'Azur, Observatoire de la Côte d'Azur, CNRS, Laboratoire Lagrange, Nice, France; [11]University of Hawai'i at Mānoa, Honolulu, HI, USA.

Introduction: The Origins, Spectral Interpretation, Resource Identification, and Security–Regolith Explorer (OSIRIS-REx) mission discovered hundreds of impact craters on (101955) Bennu [1–3]. Impact craters provide information about Bennu's surface age, geological history, and mechanical properties. A few craters contain mounds in their interiors. We use them to gain insight into Bennu's subsurface.

Observations: Three craters on Bennu larger than 10 m in diameter have mounds near their centers (Fig. 1). Smaller craters have not yet been thoroughly searched for interior mounds.) The mounds do not appear to be partially exposed or partially buried boulders. The diameters of mound craters range from ~15 to ~22 m, and the mounds are apparent in topographic profiles (Fig. 2). Mound heights range from 0.29 – 0.53 m above the crater floor. The mounds are not caused by noise in the lidar dataset. Rather, the topography exceeds the accuracy and precision of the dataset [4]. Two of the three mound craters are located on areas with low regional slopes, while the crater in Figure 1A is superposed on a ~14° regional slope. In all three cases, the mound diameter is ~0.3 times the diameter of the crater. Two additional craters may have mounds, but the topographic data are ambiguous.

Interpretations: Observations of impact craters on planetary surfaces [e.g., 5–7], as well as results from impact experiments [7] and numerical models [8], indicate that central mounds form inside craters when the floor is located near the boundary between a weak upper layer and strong substrate (e.g., lunar regolith above bedrock). The diameters of mound craters constrain the thickness of weak surface material and the depth to more competent material. Lunar examples and impact experiments [7] showed that mound craters form when the ratio between the rim-to-rim diameter of the

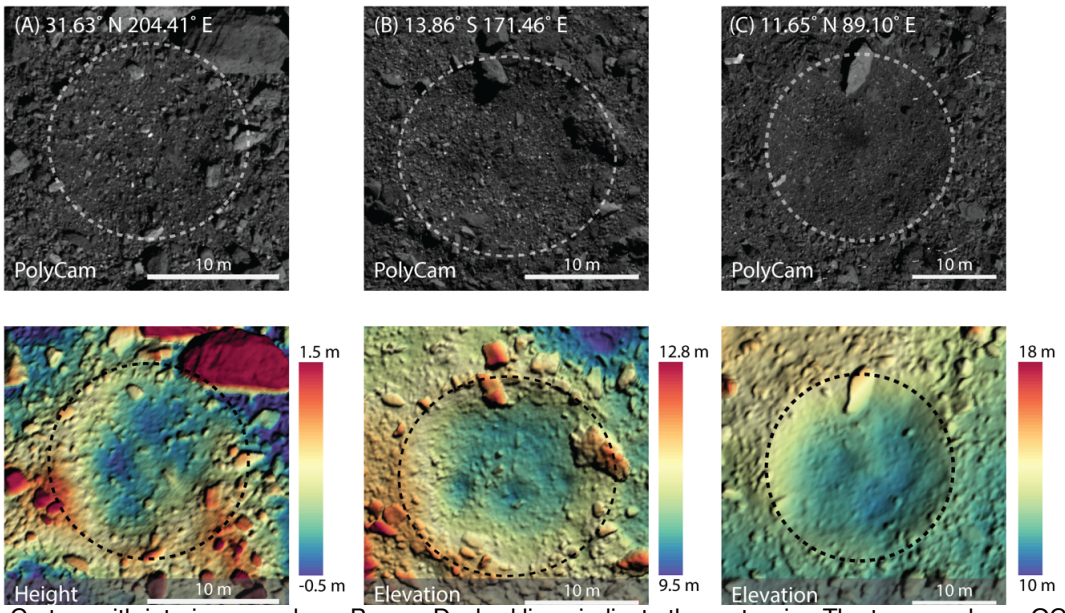

Figure 1. Craters with interior mounds on Bennu. Dashed lines indicate the crater rim. The top row shows OCAMS PolyCam images of each crater overlaid on the DTM shown in the second row. For panels B and C, the bottom row shows the DTMs colored by elevation. The crater in panel A formed on a slope. This DTM is colored by height along a normal to a plane fit to the points in the DTM. This approach emphasizes the mound by removing regional slope.

crater, D_r, and regolith thickness, t, (i.e., thickness of weaker surface material) is between ~4 and ~7.5. Applying these results to Bennu implies that the three mound craters formed in places where a layer of weak material ~2 to 6 m deep (depending on the crater) lies atop a stronger, more competent substrate. The specific ranges of D_r/t that lead to mound craters on Bennu might differ from the values determined by [7] owing to differences in material properties (e.g., strength, porosity) on Bennu vs. the Moon. However, numerical models [8] indicate that the strength contrast between the two layers, rather than the absolute strengths of the upper material or substrate, is the relevant factor in mound crater formation.

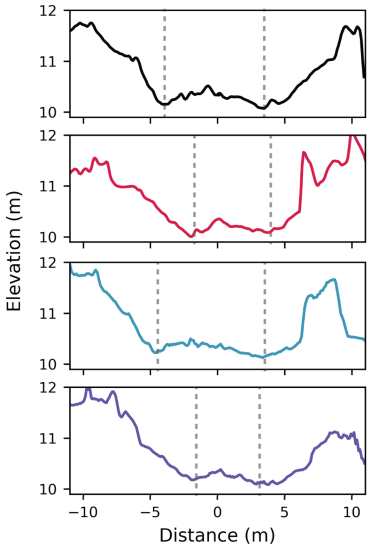

Fig. 2. Topographic profiles across the crater in Fig. 1b. Dashed lines denote the edges of the interior mound.

We hypothesize that these mound craters formed in regions underlain by a competent block or boulder. Existing analyses [e.g., 5–8] are not sufficiently detailed to pinpoint the size of the stronger substrate relative to the size of the crater, but we speculate that the stronger material would need to be wider than the crater (i.e., >15–20 m across; dozens of such boulders occur on Bennu [1,4,9]). Only a few craters have central mounds, which implies that the conditions that lead to mound formation are not widespread. On the one hand, because Bennu is a rubble pile, one might expect craters to often form above a block or boulder, which would suggest that mound craters should be common. On the other hand, mound craters can form only when the layer of weaker material is a specific thickness relative to the size of the crater [7,8], which would restrict the number of craters one would expect to contain mounds in a rubble pile. In addition, the subsurface block may need to be of a certain length scale with respect to the overlying crater or oriented subparallel to the pre-impact surface, in which case the conditions for mound crater formation would be even less common.

Discussion: Mound craters are one of several lines of evidence that suggest the properties of Bennu's interior differ from its surface. The touch-and-go (TAG) sampling event mobilized abundant material, suggesting a weak surface [14]. Based on thermal inertia, some boulders exposed at the surface of Bennu are also quite weak [10]. The Small Carry-on Impactor (SCI) experiment implied a weak surface on Ryugu [11], as does ejecta [12] associated with a crater on Bennu. Terraces on Bennu also indicate the presence of weak surface materials [13]. At the same time, in some places the subsurface is sufficiently strong to form mound craters, Bennu's interior has enough stiffness to support global-scale north-south ridges [4,9], as well as a heterogeneous mass distribution [15]. OSIRIS-REx has provided tantalizing clues to the nature of Bennu's interior—and by extension, interiors of other rubble-piles. More work is needed to understand the links between the surfaces and interiors of these small bodies.

Acknowledgments: We thank the entire OSIRIS-REx Team for making the Bennu encounter successful. This work used the Small Body Mapping Tool (sbmt.jhuapl.edu). Mound crater DTMs are available at lib.jhuapl.edu/papers/the-morphometry-of-impact-craters-on-bennu/. Data from OLA and OCAMS used here are available in the Planetary Data System [16,17]. This material is based on work supported by NASA under contract NNM10AA11C issued through the New Frontiers Program. OLA and Canadian science support were provided by a contract with the Canadian Space Agency. P.M. acknowledges support from the French space agency, CNES and from the European Union's Horizon 2020 research and innovation program under grant agreement No 870377 (project NEO-MAPP), and from Academies of Excellence: Complex systems and Space, environment, risk, and resilience, part of the IDEX JEDI of the Université Côte d'Azur.

References: [1] Walsh K. J. et al. (2019) *Nat. Geosci.* 12, 242–246. [2] Bierhaus E. B. et al. (2019) *LPS L,* Abstract #2496. [3] Bierhaus E. B. et al. (2020) *LPS LI,* Abstract #2156. [4] Daly M. G. et al. (2020) *Sci. Adv.* 6, eabd3649. [5] Bart, G. D. (2014) *Icarus* 235, 130–135. [6] Bart G. D. et al. (2011) *Icarus* 215, 485–490. [7] Quaide W. L. & Oberbeck V. R. (1968). *J. Geophys. Res.* 73, 5247–5270. [8] Senft L. E. & Stewart S. T. (2007). *J. Geophys. Res. Planets* 112. [9] Barnouin O. S. et al. (2019) *Nat. Geosci.* 12, 247. [10] Rozitis B. et al. (2020) *Sci. Adv.* 6, eabc3699. [11] Arakawa M. et al. (2020). *Science,* 368, 67 – 71. [12] Perry M. E. et al. (2019) *Asteroid Science in the Age of Hayabusa2 and OSIRIS-REx,* Abstract #2133. [13] Barnouin O. et al. (2019) EPSC-DPS2019-255. [14] Lauretta D. S. et al. (2021) this conference. [15] Scheeres D. J. et al. (2020) *Sci. Adv.* 6, eabc3350. [16] Daly, M. et al. (2019). OSIRIS-REx Laser Altimeter (OLA) Bundle, urn:nasa:pds:orex.ola. [17] Rizk, B. et al. (2019). OSIRIS-REx Camera Suite (OCAMS) Bundle, urn:nasa:pds:orex.ocams.